

Preparation and properties of stearic acid/expanded graphite composite phase change material for low-temperature solar thermal application

Haitao Yu¹ · Jianmin Gao¹ · Yao Chen¹ · Yang Zhao¹

Received: 27 April 2015 / Accepted: 4 November 2015 / Published online: 20 November 2015
© Akadémiai Kiadó, Budapest, Hungary 2015

Abstract Stearic acid (SA)/expanded graphite (EG) composite phase change material (PCM) was prepared through physical adsorption of SA to EG with mass ratios of SA varying from 6:1 to 11:1. The prepared composite PCM was characterized using scanning electron microscopy images, X-ray diffraction analysis, differential scanning calorimetry, and thermogravimetric analysis. A latent thermal energy storage system was used to measure the thermal cycling performance of the prepared composite PCM. The results show that when the composite PCM was prepared with 90 % SA, a high latent heat value and good thermal stability were achieved. Additionally, the heat transfer efficiency of both heat storage and heat retrieval was improved by the addition of EG.

Keywords Thermal energy storage · Phase change material · Expanded graphite · Stearic acid

Introduction

Over the past several decades, solar energy has become more and more commonly used as a clean and renewable natural energy source. However, it exhibits significant instability and can be harvested only intermittently due to

the influence of weather and seasonal changes. To combat these drawbacks, latent heat storage has been used as an effective method for resolving the time and space conflicts of energy supply. In particular, low-temperature solar thermal applications have received increasing attention in many fields, including solar water heating, solar drying, and building energy saving engineering [1–4].

Current research on LTES has focused on the use of organic phase change materials, mainly comprised of paraffins and fatty acids, for heat storage [5]. Many studies have explored how to improve thermal conductivity and stability while decreasing PCM leakage. For example, Zhang [6] found that expanded graphite (EG) prepared for 10 s at an irradiation power of 800 W demonstrated a maximum sorption capacity of 92 mass% with paraffin. Xia [7] conducted an experimental investigation of the EG/paraffin composite PCM with the mass fraction of EG varying from 0 to 10 mass% and found that, compared to pure paraffin, the heat storage/retrieval durations for EG(10)/paraffin(90) composite decreased by 48.9/66.5 %. Using PCMs prepared with paraffin and hybrid nanomaterials (50 % CuO–50 % TiO₂), Harikrishnan [8] found that when the composite PCM compound was comprised of 1.0 mass% of hybrid nanomaterials, PCM melting and freezing times were 29.8 and 27.7 % less than those of paraffin, respectively. In a study of EG/paraffin/organic montmorillonite (OMMT) composite PCM prepared using the melt intercalation method, Kao [9] found that using EG/paraffin/OMMT instead of paraffin strengthened heat transfer efficiency and decreased heating time to one-sixth that of paraffin. Trigui [10] used LDPE as a supporting matrix in a LDPE/wax composite PCM, which demonstrated good potential for application in a passive solar walls. Meanwhile, Jiao [11] discovered that lauric acid (LA)–stearic acid (SA) can dispersed quite evenly in the

✉ Jianmin Gao
jmgao_bjfu@163.com

✉ Yao Chen
ychen@bjfu.edu.cn

¹ MOE Key Laboratory of Wooden Material Science and Application, Beijing Key Laboratory of Wood Science and Engineering, Beijing Forestry University, Beijing 100083, China

porous skeleton of expanded perlite, producing composite PCM with high thermal stability. Studying the thermal properties of PCM filled with carbon nanofiber (CNF) and carbon nanotube (CNT), Cui [12] demonstrated that because of its superior dispersion, CNF is a more effective thermal conductive filler than CNT. Fu [13] prepared a new palmitic acid (PA)/polyaniline (PANI) form-stable PCMs were prepared by surface polymerization, the thermal conductivity could be effectively improved by Cu NWs. Fang [14] compared the properties of SA/EG composites with mass ratios 1:1, 3:1 and 5:1 and determined that there no SA leakage occurred, even when the composites were in a molten state because the thermal diffusivity of the composites was 10 times higher than that of SA alone. Using the sol–gel method, Li [15] prepared a form-stable paraffin/silicon dioxide/EG composite PCM with a phase change temperature of 27.72 °C and a latent heat of 104.4 J g⁻¹. Li also reported on PCM produced by absorbing capric-palmitic acid into attapulgite using the vacuum method, which exhibited a phase change temperature of 21.71 °C and a latent heat is 48.2 J g⁻¹ [16]. Lastly, Wang [17] prepared a novel sebacic acid/EG composite PCM for use in medium-temperature solar thermal storage, as the low extent of subcooling inherent in sebacic acid is prevented by the combination of sebacic acid and EG.

Despite the innovations made in the studies described above, the majority of researchers have continued to use paraffin as latent heat storage material in low-temperature solar heat storage systems. Other organic PCMs that are suitable for use in low-temperature heating systems (40–75 °C) require further investigation. Therefore, this study focuses the preparation of a novel potential PCM for low-temperature heating systems, such as those used in solar drying and solar water heating. SA/EG composite PCMs with mass ratios varying from 6:1 to 11:1 were prepared, and the optimum ratio of PCM composite was determined using analysis of both structural and thermal properties. The heat storage/release characteristics of the SA/EG composite PCM were studied using an LTES system and compared with those of SA.

Experimental

Materials and sample preparation

SA (Analytical Reagent, Xilong Chemical Co., Ltd., China) was used without further purification. To prepare EG, graphite powders (80 meshes, expandable volume: 600 mL g⁻¹, Qingdao Jinrilai Graphite Co., Ltd., China) were dried in a vacuum oven for 12 h at 60 °C, following which the powers were treated for 60 s in a furnace set at 800 °C [18].

Preparation and characterization of the composites

The different mass ratios of SA and EG, 6:1(PCM 1), 7:1(PCM 2), 8:1(PCM 3), 9:1(PCM 4), 10:1(PCM 5) and 11:1(PCM 6) were mixed for 20 min using mechanical stirring. The samples were placed in a vacuum oven for 12 h at 90 °C in pressure of 0.1 MPa and stirred every 2 h. After the samples were cooled to room temperature, the SA/EG composite PCMs were constructed. To ensure that the PCMs were functional, the liquid leakage test was performed according to the method developed by Yang et al. [19].

The morphologies and microstructures of both EG and the SA/EG composites were observed using a scanning electron microscope (SEM, JSM-7001F, Japan). The crystalline phases of SA, EG, and the SA/EG composite PCMs were characterized using X-ray diffraction (D8-ADVANCE, Bruker, Germany). The phase change temperature and latent heats of SA and the SA/EG composites were obtained with a differential scanning calorimeter (Q2000, TA, USA). The tests were carried out under a constant stream of nitrogen at a flow rate of 20 mL min⁻¹ and a heating/cooling rate of 5 °C min⁻¹ from room temperature to 90 °C. The thermal stability of SA and the SA/EG composite samples were investigated using thermogravimetric analysis performed with a thermal analyzer (TGA/DSC1/1600HT, Mettler-Toledo, Switzerland). During the thermal stability tests, the samples were heated from room temperature to 400 °C at a rate of 20 °C min⁻¹ under a nitrogen atmosphere with a flow rate of 50 mL min⁻¹.

Thermal energy storage performance testing device

The LTES system consists of a cylindrical storage unit, a constant temperature water bath, three thermocouples (PT100), and a data acquisition unit (M400). A schematic diagram of the LTES system is shown in Fig. 1. The cylindrical storage unit (stainless steel, inner diameter 60 mm, height 120 mm, and wall thickness 1 mm) was filled to a height of 90 mm with SA and the PCM, with the remaining 30 mm left empty to accommodate the volume increase of

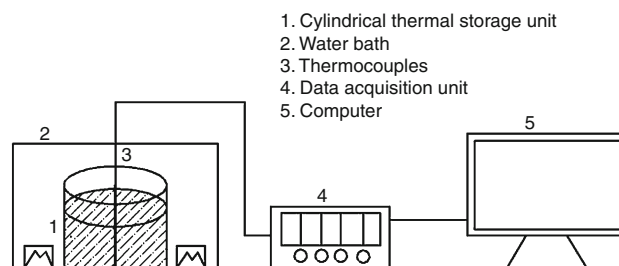


Fig. 1 Schematic of the LTES system

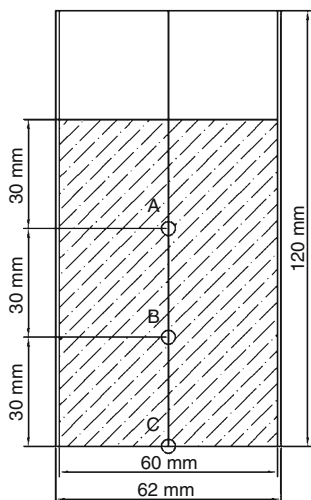


Fig. 2 Cylindrical thermal storage unit

the PCM during melting. As shown in Fig. 2, to measure the change in inner temperature of SA and the PCM, three thermocouples were decorated in a row on the center axis of the storage unit. The temperature of water bath was set at 70 °C to ensure that the heat storage material melted completely during the heat storage process. The retrieval process was performed at room temperature. The temperature variations of SA and the PCM during heat storage and retrieval were collected using the data acquisition unit.

Results and discussion

Structure properties of SA/EG composite

Figure 3 shows the SEM images of EG and the SA/EG PCMs. It can be seen from Fig. 3a that the EG exhibits a porous particle structure, where melted SA can be adsorbed. Examining the microstructure of the composite PCM 1 in Fig. 3b, it can be observed that SA is completely adsorbed in the pores of EG, but voids not filled with SA still exist. With increase in mass fraction of SA, the amount of the empty pores remaining in EG gradually decreases. As shown in Fig. 3c, the honeycomb-like network of the EG surface is thoroughly covered with an SA layer with PCM 4 and, at this degree of mass fraction, little superfluous stearic acid is visible in the image. Unfortunately, the presence of superfluous stearic acid is clearly observable in with PCM 6, shown Fig. 3d. Meanwhile, on the basis of the liquid leakage tests performed on PCM 5 and PCM 6, PCMs with mass ratios of SA to EG increased to 10:1 and 11:1 experience leaking. From the analysis above, it can be concluded that PCM composites with 90 mass% SA (PCM 4) can be expected to be well encapsulated.

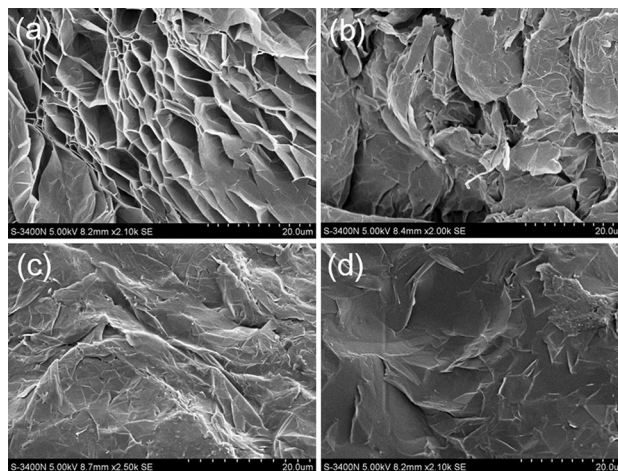


Fig. 3 SEM photographs of the a EG, b PCM 1, c PCM 4 and d PCM 6

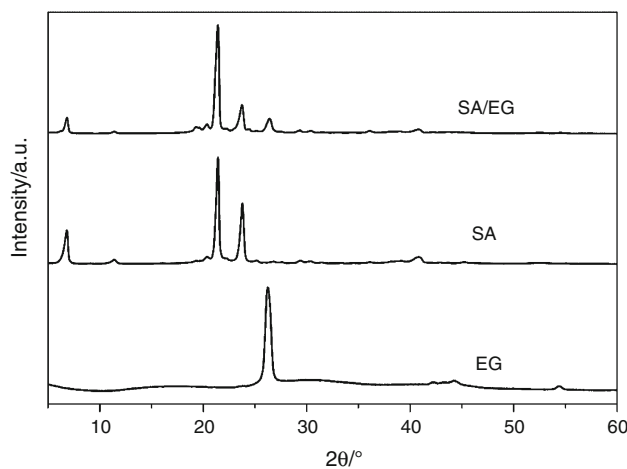


Fig. 4 XRD patterns of EG, SA, and the SA/EG composite PCM

The XRD patterns of SA, EG, and the SA/EG composite PCM are shown in Fig. 4, from which it can be seen that the diffraction peaks of SA occur at 6.8°, 21.4°, and 23.7°. EG exhibits one strong diffraction peak located at 26.2°, which can be attributed to the feature peak (002) of graphite. The XRD peaks of the composites occur at 6.8°, 21.4°, 23.7°, and 26.2°, containing all the peaks of both SA and EG; therefore, it follows that this is a physical change, not a chemical one. Prepared through physical adsorption only, the composite PCMs maintain the heat storage performance and chemical properties of SA.

Thermal properties of the SA/EG composites

The differential scanning calorimetry (DSC) curves of SA and the SA/EG composite PCMs are shown in Fig. 5. The corresponding thermal characteristics of these samples are summarized in Table 1. A high latent heat storage capacity

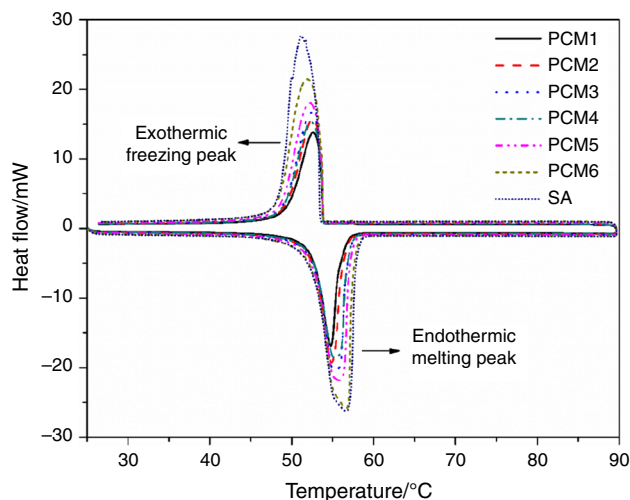


Fig. 5 DSC curves of the SA and the SA/EG composite PCMs

is important to low-temperature solar thermal application, and it is clear from the data that though the latent heat values of all the SA/EG composites are reduced by the addition of EG to pure SA, the latent heat values of SA/EG remain more than acceptable. PCM 6 and PCM 5 exhibited higher latent heat values; however, liquid leakage occurred. The melting points of the PCMs decreased and the solidifying points increased due to increased heat transfer caused by adding EG, which has high thermal conductivity. The melting and freezing phase change temperatures and latent heats of PCM 4 were 52.74 and 53.70 °C and 169.90 and 166.10 J g⁻¹, respectively, indicating its potential for application in low-temperature solar thermal systems based on its melting temperature and high latent heat properties.

Figure 6 shows the DSC curves of PCM 4 before and after experiencing 500 and 1000 heating-cooling cycles, and the corresponding thermal characteristics of these samples are summarized in Table 2. It can be seen that there is no obvious difference in the melting onset temperature, while a slight reduction in the melting peak temperature from 56.33 to 55.16 °C is observed. Both the solidifying onset temperature and the solidifying peak

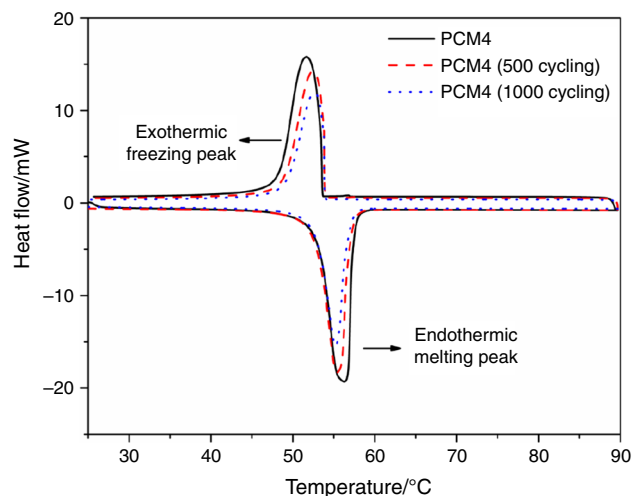


Fig. 6 DSC curves of the PCM 4 before and after experiencing 500 and 1000 heating-cooling cycles

temperature increase slightly from 53.70 to 53.90 °C and from 51.58 to 52.62 °C, respectively. Moreover, the melting and solidifying latent heats of PCM 4 after experiencing 500 heating-cooling cycles are 163.3 and 158.7 J g⁻¹, which dropping by 3.9 and 4.5 % respectively. The melting and solidifying latent heats of PCM 4 after experiencing 1000 heating-cooling cycles are 161.8 and 156.1 J g⁻¹, which dropping by 4.8 and 6.0 % respectively. The results obtained from the heating-cooling cycling tests indicate that PCM 4 exhibits good cycle thermal stability.

Thermal stability of the SA/EG composites

Figure 7 exhibits the thermogravimetric (TG) and derivative thermogravimetric (DTG) curves of SA and the SA/EG composite PCMs. From the figures, it can be seen that the 5 % mass loss temperature ($T_{-5\text{mass}\%}$) of PCM is 226 °C, higher than that of pure SA (208 °C). The onset temperature of mass loss (T_{onset}) and the temperature of maximum mass loss rate (T_{max}) of the EG/SA composite PCM are 254

Table 1 DSC data of the SA and the SA/EG composite PCMs

Samples	Melting			Solidifying		
	Onset temperature/°C	Peak temperature/°C	Latent heat/J g ⁻¹	Onset temperature/°C	Peak temperature/°C	Latent heat/J g ⁻¹
SA	52.81	56.62	184.30	52.96	51.15	177.90
PCM 1	52.66	55.86	165.10	53.77	52.20	158.20
PCM 2	52.70	56.04	166.40	53.76	51.92	163.20
PCM 3	52.73	56.16	167.60	53.74	51.71	164.30
PCM 4	52.74	56.33	169.90	53.70	51.58	166.10
PCM 5	52.76	56.41	171.50	53.68	51.46	167.20
PCM 6	52.77	56.53	173.60	53.66	51.32	168.60

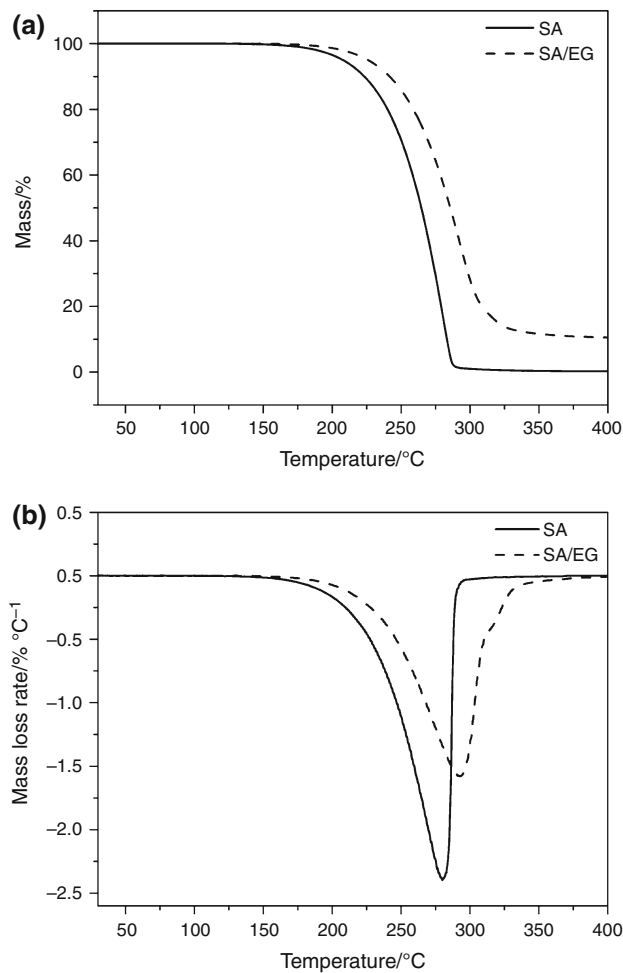


Fig. 7 **a** TG curves and **b** DTG curves of SA and SA/EG composite PCM

and 293 °C, respectively, both higher than those of SA (246 and 280 °C, respectively). This demonstrates that the addition of EG positively improves the thermal stability of the composite PCMs. Overall, the results reveal that the PCMs exhibit good thermal stability and satisfy the operating range requirements of low-temperature thermal storage systems.

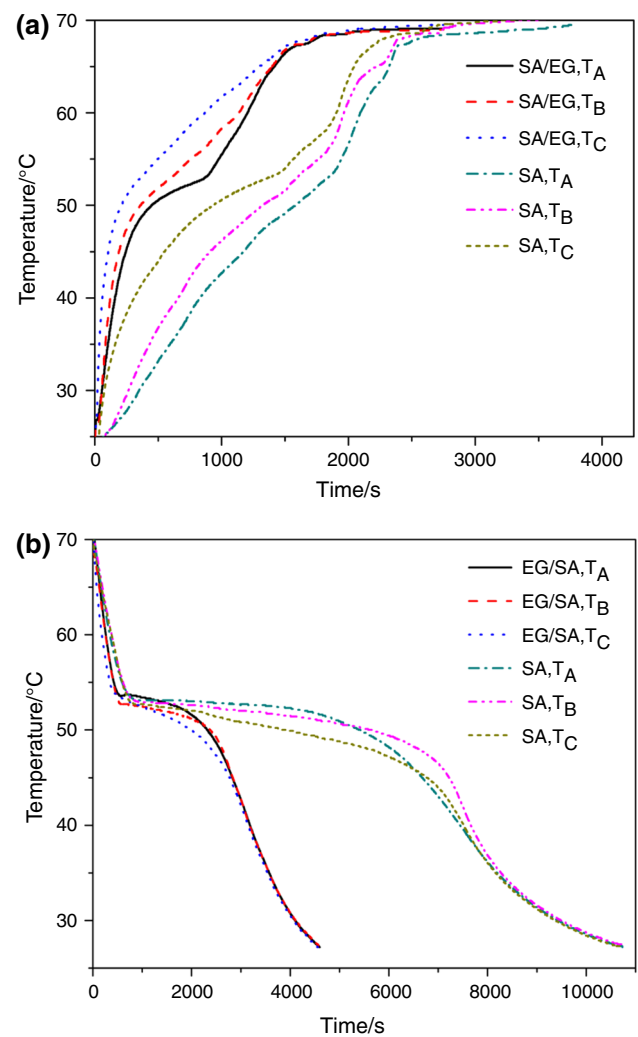


Fig. 8 Temperature evolutions of the heat storage unit during **a** heat storage and **b** retrieval

Heat storage/retrieval performance of SA and the SA/EG in an LTES system

The temperature evolutions of the LTES unit with pure SA and with the SA/EG composite during heat storage

Table 2 DSC data of PCM 4 before and after thermal cycling

Samples	Melting			Solidifying		
	Onset temperature/°C	Peak temperature/°C	Latent heat/J g ⁻¹	Onset temperature/°C	Peak temperature/°C	Latent heat/J g ⁻¹
PCM 4	52.74	56.33	169.90	53.70	51.58	166.10
PCM 4 (after 500 cycles)	52.82	55.39	163.3	53.85	52.42	158.7
PCM 4 (after 1000 cycles)	52.72	55.16	161.8	53.90	52.62	156.1

and heat retrieval are shown in Fig. 8. The heat storage process took 2759 s with SA and 1798 s with the composite PCM, while the heat retrieval process took 10,737 s with SA and 4585 s with the PCM. The time required for heat storage/retrieval with the PCM decreased by 34.8 and 57.3 %, respectively, compared to SA. This suggests that the heat storage/retrieval cycle of the composite PCM was decreased by the addition of EG and that the efficiency of heat transfer was likewise improved. Comparing degree of reduction in time required for heat storage/retrieval using SA/EG composite, it can be observed that heat transfer efficiency is more apparent in the heat retrieval process than it is in the heat storage process. This is due to the fact that natural convection plays an important role in the heat storage process, whereas heat transfer is primarily dependent on thermal conduction. As SA is adsorbed in the pores of EG, its thermal conductivity is greatly improved, while natural convection is restricted.

Conclusions

In this study, SA/EG composite PCMs were prepared with different mass ratios and the properties of the PCMs investigated and compared to those of pure SA. The porous, networked structure of EG was found to uniformly adsorb SA when the optimal mass percentage of SA in the SA/EG composite PCM is approximately 90 %. That this integration of SA and EG was simply physical and occurred without any chemical interaction was verified. The melting and freezing phase change temperatures and latent heats of the optimal PCM were 52.74 and 53.70 °C and 169.90 and 166.10 J g⁻¹, respectively. The PCM just changed slightly in phase change temperature and latent heat after 500 and 1000 heating–cooling cycles, showing a good cycle thermal stability. A heat storage/retrieval test of SA and the SA/EG composite in a latent thermal energy storage system revealed that using the SA/EG composite reduced the time required for heat storage/retrieval by 34.8/57.3 %. TG analysis showed that the PCM exhibited good thermal stability. On the whole, the composite PCM demonstrates strong potential for use in low-temperature solar thermal heat storage systems, mainly due to its suitable melting temperature, high latent heat value, and heat transfer efficiency.

Acknowledgements Financial support from the Fundamental Research Funds for the Central Universities (YX2014-03), the National Natural Science Foundation of China (series Project No. 31400498), and the Scientific Research Foundation for Returned Overseas Scholars, Ministry of Education of China (No. 14JIX-01) are gratefully acknowledged.

References

1. Mahfuz MH, Anisur MR, Kibria MA, Saidur R, Metselaar IHSC. Performance investigation of thermal energy storage system with Phase Change Material (PCM) for solar water heating application. *Int Commun Heat Mass Transf.* 2014;57:132–9.
2. VijayaVenkataRamana S, Iniyamb S, Goic R. A review of solar drying technologies. *Renew Sustain Energy Rev.* 2012;16: 2652–70.
3. Shringi V, Kothari S, Panwar NL. Experimental investigation of drying of garlic clove in solar dryer using phase change material as energy storage. *J Therm Anal Calorim.* 2014;118:533–9.
4. Kalnaes SE, Jelle BP. Phase change materials and products for building applications: a state-of-the-art review and future research opportunities. *Energy Build.* 2015;94:150–76.
5. Pielichowska K, Pielichowski K. Phase change materials for thermal energy storage. *Prog Mater Sci.* 2014;65:67–123.
6. Zhang Z, Zhang N, Peng J, Fang X, Gao X, Fang Y. Preparation and thermal energy storage properties of paraffin/expanded graphite composite phase change material. *Appl Energy.* 2012;91:426–31.
7. Xia L, Zhang P, Wang RZ. Preparation and thermal characterization of expanded graphite/paraffin composite phase change material. *Carbon.* 2010;48:2538–48.
8. Hari Krishnan S, Deepak K, Kalaiselvam S. Thermal energy storage behavior of composite using hybrid nanomaterials as PCM for solar heating systems. *J Therm Anal Calorim.* 2014;115:1563–71.
9. Kao H, Li M, Lv X, Tan J. Preparation and thermal properties of expanded graphite/paraffin/organic montmorillonite composite phase change material. *J Therm Anal Calorim.* 2012;107:299–303.
10. Trigui A, Karkri M, Krupa I. Thermal conductivity and latent heat thermal energy storage properties of LDPE/wax as a shape-stabilized composite phase change material. *Energy Convers Manag.* 2014;77:586–96.
11. Jiao C, Ji B, Fang D. Preparation and properties of lauric acid-stearic acid/expanded perlite composite as phase change materials for thermal energy storage. *Mater Lett.* 2012;67:352–4.
12. Cui Y, Liu C, Hu S, Yu X. The experimental exploration of carbon nanofiber and carbon nanotube additives on thermal behavior of phase change materials. *Sol Energy Mater Sol Cells.* 2011;95:1208–12.
13. Fu R, Zhang L, Zeng J, Zhu L, Zhu Z, Zhu X, Li R, Xiao Z, Cao Z. Preparation and thermal properties of palmitic acid/polyaniline/copper nanowires form-stable phase change materials. *J Therm Anal Calorim.* 2014;115:1133–41.
14. Fang G, Li H, Chen Z, Liu X. Preparation and characterization of stearic acid/expanded graphite composites as thermal energy storage materials. *Energy.* 2010;35:4622–6.
15. Li M, Wu Z, Tan J. Properties of form-stable paraffin/silicon dioxide/expanded graphite phase change composites prepared by sol–gel method. *Appl Energy.* 2012;92:456–61.
16. Li Min, Zhishen Wu, Kao Hongtao. Study on preparation, structure and thermal energy storage property of capric-palmitic acid/attapulgit composite phase change materials. *Appl Energy.* 2011;88:3125–32.
17. Wang S, Qin P, Fang X, Zhang Z, Wang S, Liu X. A novel sebacic acid/expanded graphite composite phase change material for solar thermal medium-temperature applications. *Sol Energy.* 2014;99:283–90.
18. Sari A, Karaipekli A. Preparation, thermal properties and thermal reliability of palmitic acid/expanded graphite composite as form-stable PCM for thermal energy storage. *Sol Energy Mater Sol Cells.* 2009;93:571–6.
19. Yang X, Yuan Y, Zhang N, Cao X, Liu C. Preparation and properties of myristic-palmitic-stearic acid/expanded graphite composites as phase change materials for energy storage. *Sol Energy.* 2014;99:259–66.